Bootstrap Percolation on Random Geometric Graphs

Milan Bradonjić and Iraj Saniee

Mathematics of Networks and Communications
Bell Laboratories, Alcatel-Lucent
600 Mountain Avenue, Murray Hill, NJ 07974, USA
{milan,iis}@research.bell-labs.com

Abstract

Bootstrap percolation has been used effectively to model phenomena as diverse as emergence of magnetism in materials, spread of infection, diffusion of software viruses in computer networks, adoption of new technologies, and emergence of collective action and cultural fads in human societies. It is defined on an (arbitrary) network of interacting agents whose state is determined by the state of their neighbors according to a threshold rule. In a typical setting, bootstrap percolation starts by random and independent "activation" of nodes with a fixed probability p, followed by a deterministic process for additional activations based on the density of active nodes in each neighborhood (θ activated nodes). Here, we study bootstrap percolation on random geometric graphs in the regime when the latter are (almost surely) connected. Random geometric graphs provide an appropriate model in settings where the neighborhood structure of each node is determined by geographical distance, as in wireless *ad hoc* and sensor networks as well as in contagion. We derive tight bounds on the critical threshold, $p_c(\theta)$, such that for all $p > p_c(\theta)$ full percolation takes place, whereas for $p < p_c(\theta)$ it does not. We conclude with simulations that compare numerical thresholds with those obtained analytically.

1 Introduction

Some crystals or lattices studied in physics and chemistry can be modeled as consisting of atoms occupying sites with specified probabilities. The lattice as a whole would then exhibit certain macroscopic properties, such as (ferro)magnetism, only when a sufficient number of neighboring sites of each atom are also similarly occupied. In computer memory arrays each functional memory unit can be considered as an occupied site, and a minimum percentage of functioning units are needed in the vicinity of

each memory unit in order to maintain the array with proper functioning. In adoption of new technology or emergence of cultural fads, an individual is positively influenced when a sufficient number of its close friends have also done so.

All three examples cited above may be modeled via a formal process called "bootstrap percolation" which is a dynamic process that evolves similar to a cellular automaton. Unlike cellular automata, however, this process can be defined on arbitrary graphs and starts with random initial conditions. Nodes are either active or inactive. Once activated, a node remains active forever. Each node is initially active with a (given) probability p. Subsequently and at each discrete time step, a node becomes active if θ of its nearest neighbors are active, for a fixed value of $\theta = 1, 2, 3, \ldots$. As time evolves, a fraction Φ of all the nodes are activated. The emergence of macroscopic properties of interest typically involve Φ to be at or close to 1.

Gersho and Mitra [11] studied a similar model for adoption of new communication services using a random regular graph and obtained (implicit) critical thresholds for widespread adoption. Chalupa *et al* [8] were the first to introduce bootstrap percolation formally to explain ferromagnetism. Their analysis is carried out on regular trees (Bethe lattices) and a fundamental recursion is derived for computation of the critical threshold that has since been used extensively. In the more recent past, results for non-regular (infinite) trees have also been derived by Balogh *et al* [5]. Aizenman and Lebowitz [1] studied metastability of bootstrap percolation on the d-dimensional Euclidean lattice $\mathbb{Z}^d$ which has now been thoroughly investigated in two and three dimensions, see [7, 16]. The existence of a sharp metastability threshold for bootstrap percolation in two-dimensional lattices was proved by Holroyd [16] and recently generalized to d-dimensional lattices by Balogh *et al* [4]. Even more recently, bootstrap percolation has been studied on random graphs $G(n, p)$ by Luczak *et al* [18]. In [24] Watts proposed a model of formation of opinions in social networks in which the percolation threshold is a certain fraction of the size of each neighborhood rather than a fixed value, a departure from the standard model that is used by Amini in [2] for random graphs with a given degree sequence.

Many diffusion processes of interest have a *physical contact* element. A link in an *ad hoc* wireless network, a sensor network, or an epidemiological graph connotes physical proximity within a certain locality. Study of diffusion of virus spread in *ad hoc* wireless, sensor or epidemiological graphs requires this notion of neighborhood for accurate estimation of likelihood of full percolation. This is in contrast to models with long-range reach where physical proximity plays little, if any, role. The natural random model for such phenomena is the random geometric graph. In this work, we focus on bootstrap percolation on random geometric graphs, a topic that has not been investigated, to the best of our knowledge, and obtain tight bounds on their critical thresholds for full percolation.

2 Random Geometric Graph Model

One of the transitions from the random graph model $G(n,p)$ of Erdős and Rényi [9, 10] and Gilbert [12] to models that may describe processes constrained by geometric distances among the nodes is the model of random geometric graphs (RGGs) by Gilbert [13]. The RGG model has been used in many disciplines: for modeling of wireless sensor networks [22], cluster analysis, statistical physics, hypothesis testing, spread of computer viruses in wired networks, processes involving physical contact among individuals, as well as other related disciplines, see [21] for more details. For example, a wireless sensor network typically contains a large number of randomly deployed nodes with links determined by geometric proximity enabled by (a small) radio range among the nodes that is sufficient to enable successful signal transmission across the network. A further application of RGG is in representing d-attribute data where numerical attributes are used as coordinates in $\mathbb{R}^d$ and two nodes are considered connected if they are within a threshold (Euclidean) distance r of each other. The metric distance imposed on such a RGG captures the similarity between data elements.

Consider an RGG in two dimensions that is constructed by drawing n nodes uniformly at random within $[0,1]^2$ and connecting every pair of nodes at Euclidean distance at most r. Let us denote this process by RGG(n,r). A summary of basic structural properties of RGG(n,r) is as follows.

(i) RGG(n,r) is a 'homogeneous' geometrical model where the distribution of the number of nodes within a distance r from a given node follows the same binomial distribution $\mathrm{Bin}(n-1, r^2\pi)$ (with appropriate correction when the center is within a distance r of the boundary). The average degree $D = \mathbb{E}(\deg)$ of a node is $r^2\pi$ in the limit.

(ii) There is a *critical value* λ_c such that for $r > \sqrt{\lambda_c/n}$ there exists a *giant component*, i.e., the largest connected component of order $\Theta(n)$ nodes contained in RGG(n,r) whp[1], [21]. We denote the critical threshold for existence of a giant component by $r_c := \sqrt{\lambda_c/n}$.

(iii) In this regime, the second largest component is of order $\mathcal{O}(\ln^2 n)$.

(iv) The exact theoretical value of the constant λ_c is not known. It is experimentally established that $\lambda_c \approx 1.44$ for the dimension $d = 2$ [23], while theoretical bounds $\lambda_c \in [0.696, 3.372]$ are given in [19]. There has been a recent improvement of the lower bound $\lambda_c > 4/(3\sqrt{3}) \approx 0.7698$ [17].

[1]Whp or "with high probability", means with probability one as n, the number of nodes, tends to infinity.

(v) RGG(n, r) is connected whp for $r > \sqrt{\ln n/\pi n}$, [15, 20]. We denote the critical threshold for connectedness by $r_t := \sqrt{\ln n/\pi n}$.

(vi) Every monotone property in a RGG(n, r) (e.g., existence of a giant component and connectedness) exhibits a sharp threshold [14].

In order to simplify our analysis on RGGs, we now introduce $G_{n,r}$ which is asymptotically isomorphic to RGG$(n, rn^{-1/2})$. Let $\mathcal{X}$ be a Poisson point process of intensity 1 on $\mathbb{R}^2$. Consider points of $\mathcal{X}$ contained in $[0, \sqrt{n}]^2$ representing the nodes of a graph denoted $G_{n,r}$. Two nodes of $G_{n,r}$ are connected if their Euclidean distance is at most r. Our analysis from here on will be based upon the fact that an instance of $G_{n,r}$ is isomorphic to an instance of RGG$(n, rn^{-1/2})$ whp [21].

We parameterize $r = \sqrt{\pi^{-1} a \ln n}$ by introducing a new parameter a which measures how denser $G_{n,r}$ is compared to an instance G_{n,r_t} at the threshold for connectedness r_t. The condition $a > 1$ enables us to deal with an asymptotically connected $G_{n,r}$ [15, 21]. Notice that for sufficiently large n the expected degree is concentrated around its mean $a \ln n$, which can be easily derived from the Chernoff and union bounds.

For $n = 1000$, the critical thresholds for the existence of a giant component and connectedness in $G_{n,r}$ satisfy $r_c \approx 0.0316$ and $r_t \approx 0.0469$, respectively. In Figure 1 and Figure 2, we present $G_{n,r}$ for four different regimes when r takes values: $0.020, 0.035, 0.045, 0.050$, respectively. The values 0.020 and 0.035 correspond to 'ultra'-sparse regime and emergence of a giant component, Figure 1. The values 0.045 and 0.050 correspond to 'almost'-connected and connected regimes, Figure 2.

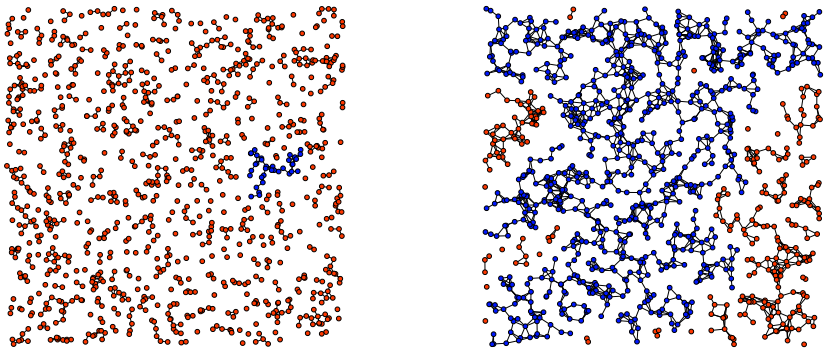

Figure 1: 'Ultra'-sparse regime and the emergence of the giant component.

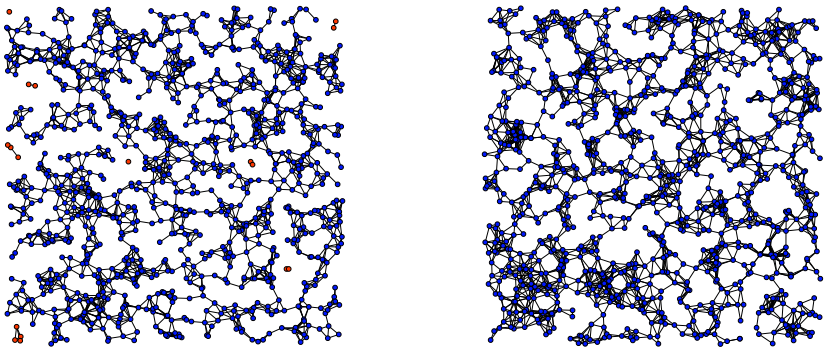

Figure 2: 'Almost'-connected and connected regimes.

3 Bootstrap Percolation

Bootstrap percolation (BP) is a cellular automaton defined on an underlying graph $G = (V, E)$ with state space $\{0, 1\}^V$ whose initial configuration is chosen by a Bernoulli product measure. In other words, every node is in one of two different states 0 or 1 (*inactive* or *active* respectively), and a node becomes active with probability p independently of other nodes within the initial configuration.

After drawing an initial configuration at time $t = 0$, a discrete time deterministic process updates the configuration according to a local rule: an inactive node becomes active at time $t+1$ if the number of its active neighbors at t (not necessarily the nearest ones) is greater than some defined *threshold* θ. Once an inactive node becomes active it remains active forever. A configuration that does not change at the next time step is a *stable* configuration. A configuration is *fully active* if all its nodes of are active.

An interesting phenomenon to study is metastability near a first-order phase transition. Do there exist p_c' and p_c'' such that:

$$\left(\forall p < p_c'\right) \lim_{t\to\infty} \mathbb{P}_p\left(V \text{ becomes fully active}\right) = 0\,,$$

and

$$\left(\forall p > p_c''\right) \lim_{t\to\infty} \mathbb{P}_p\left(V \text{ becomes fully active}\right) = 1\,?$$

A study of BP on a regular infinite tree first appeared in [8]. Subsequently, the relations between the branching number of an infinite (non-regular) tree, threshold value, and p necessary to fully percolate the tree were studied in [5].

An example of BP is a d-dimensional lattice $\mathbb{Z}^d$ equipped with Bernoulli product measure with $\theta = d$ [1]. For $\mathbb{Z}^d$ and $V = [0, L-1]^d$ the existence of a unique threshold p_c was shown in [1]. Concretely for $\mathbb{Z}^2$ and $V = [0, L-1]^2$ the exact threshold value is $p_c = \pi^2/(18 \ln L)$ [16]. Furthermore the sharp threshold for bootstrap percolation in $\mathbb{Z}^d$ in all dimensions was provided in [4].

Additionally to BP on trees and lattices, there has been recent work of BP on random regular graphs [6], Erdős-Rényi random graphs [18], as well as random graphs with a given degree sequence where the threshold depends upon node degree [2].

3.1 Bootstrap Percolation on Connected RGGs

The structure of $G_{n,r}$ is conducted by random positions of its nodes and radius $r = r(n)$; so it is more 'irregular' than the structure of a tree or a lattice. In this work we are interested in BP on $G_{n,r}$ which for brevity we denote by $BP(G_{n,r}, p, \theta)$. In this process a node becomes active with probability p independently of other nodes in the initial configuration and an inactive node becomes active at the following time step if at least $\theta = \gamma D$ of its neighbors are active, where $\gamma = \gamma(n)$ and $D(n) = \mathbb{E}(\deg) = r^2\pi = a \ln n$ is the expected node degree.

We derive critical thresholds $p'_c(\theta)$ and $p''_c(\theta)$ in $BP(G_{n,r}, p, \theta)$ such that a connected $G_{n,r}$ does not become fully active for $p < p'_c$ whp, and conversely, becomes fully active for $p > p''_c$ whp. These bounds are schematically presented in Figure 3. One of the key contributions of this work is that we show $p'_c = p''_c$.

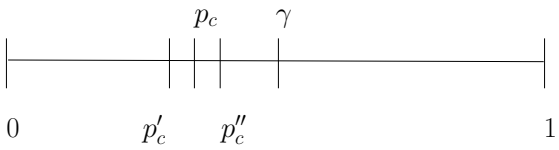

Figure 3: Critical bounds.

The main ideas of the proofs are as follows. We obtain the distribution of the number of active neighbors for each node at the initial configuration. For $p < p_c$ we use the Poisson tail bound and the union bound (see (12) in Appendix) to show that an initial configuration is stable whp. For $p > p_c$ we use the Bahadur-Rao theorem to lower bound the number of active neighbors for each node. Then we develop a geometric argument to show that a stable, fully active, configuration is reached within $\mathcal{O}(n/r)$ steps whp. This geometric argument leverages the following simple observation about BP in $\mathbb{Z}^2$ with $\theta = 1$.

Lemma 1 *Consider BP in $\mathbb{Z}^2$ with the threshold $\theta = 1$ and the initial probability p. For any N and $p = \omega(1/\sqrt{N})$, a square $[0, N]^2$ becomes fully active within $\mathcal{O}(N)$*

steps whp.

We now provide bounds on the critical threshold on p in Theorem 2 and Theorem 3.

Theorem 2 *Consider bootstrap percolation $BP(G_{n,r}, p, \theta)$ where $r = \sqrt{\pi^{-1} a \ln n}$ and $\theta = \gamma a \ln n$, for $a > 1$. For any $\gamma > 0$ and $p < p'_c(\theta) := p_c = \gamma / J^{-1}(1/a\gamma)$ where $J(x) = \ln x + x^{-1} - 1$ for $x \geqslant 1$, $G_{n,r}$ does not become fully active whp.*

Proof We show that for the conditions of the assertion, an initial configuration is stable. The number of active nodes in the initial configuration follows Poisson distribution $\mathrm{Po}(pn)$. The degree distribution of a node is $\mathrm{Po}(r^2\pi) - 1$, and the expected degree $D = r^2\pi = a \ln n$. By the thinning theorem [21] the number of active neighbors in the initial configuration follows $\mathrm{Po}(pD) - 1$. Consider the definition of the dynamics in $BP(G_{n,r}, p, \theta)$. The probability that a node becomes active at the next time step given that it is inactive initially is

$$\mathbb{P}\left(\mathrm{Po}(pD) - 1 \geqslant \gamma D\right) \quad \leqslant \quad \mathbb{P}\left(\mathrm{Po}(pD) \geqslant \gamma D\right) . \tag{1}$$

Let us now consider (1). For $p > \gamma$, given that $pD \to \infty$, the tail bound on a Poisson random variable (12) implies for any node $\mathbb{P}\left(\mathrm{Po}(pD) - 1 \geqslant \gamma D\right) \to 1$, hence for sufficiently large n an initial configuration becomes fully active whp. Therefore we consider the case $p < \gamma$ and seek a maximal $p'_c < \gamma$ (see Figure 3) such that $BP(G_{n,r}, p'_c, \gamma)$ does not become fully active whp. From (12) it follows

$$\mathbb{P}\left(\mathrm{Po}(pD) \leqslant \gamma D\right) \leqslant \exp(-pDH(\gamma/p + D^{-1})) , \tag{2}$$

where $H(x) = x \ln x - x + 1$ for $x > 0$. Moreover, the same inequality (12) yields that the number of nodes $\mathrm{Po}(n)$ within the square $[0, \sqrt{n}]^2$ is concentrated around its mean n whp. Hence the union bound over all nodes yields

$$\mathbb{P}_p\left(\text{the initial configuration is stable}\right) \geqslant 1 - \exp\left((1+\epsilon)\ln n - pDH(\gamma/p + D^{-1})\right) . \tag{3}$$

It follows that $\mathbb{P}_p\left(\text{the initial configuration is stable}\right) \to 1$ for $(1+\epsilon)\ln n - pDH(\gamma/p + D^{-1}) \to -\infty$, or equivalently $1 + \epsilon < apH(\gamma/p + D^{-1})$. The function $H(x)$ is increasing and for any $\epsilon > 0$ and sufficiently large n we have $1 + \epsilon < apH(\gamma/p) < apH(\gamma/p + D^{-1})$. Hence the following condition $1 - paH(\gamma/p) < 0$ suffices that the initial configuration is stable whp.

Consider now the function $x^{-1}H(x) = \ln x + x^{-1} - 1$ defined on $(0, \infty)$, which is monotonically decreasing on $(0, 1)$, monotonically increasing on $(1, \infty)$ and attains its minimum 0 at $x = 1$. Hence for any positive $\gamma < \infty$ there are two solutions of $x^{-1}H(x) = 1/a\gamma$, which we call $x_1 < 1 < x_2$. This yields $p > \gamma/x_1 > \gamma$ or $p < \gamma/x_2 < \gamma$. The acceptable solutions is $p < \gamma/x_2$, since $p < \gamma$.

The function $J(x) = x^{-1}H(x)$ for $x \geqslant 1$, plotted in Figure 4, is continuous and strictly increasing with the inverse $J^{-1} : [0, \infty) \to [1, \infty)$. For $J(\gamma/p) > 1/a\gamma$ the probability given in (3) tends to 1 as n tends to infinity. Finally, a bound on p is given by

$$p < \frac{\gamma}{J^{-1}(1/a\gamma)},$$

which concludes the proof. □

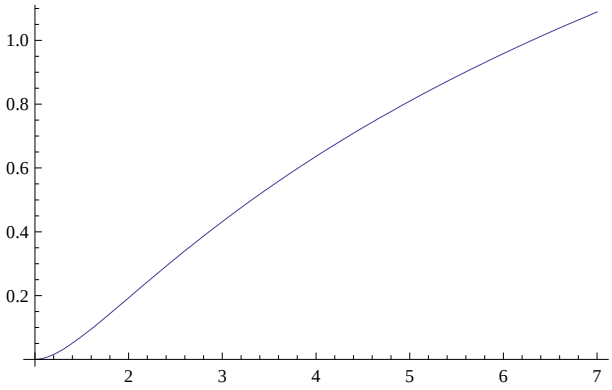

Figure 4: Function $J(x)$.

Let us denote the value $p_c(a, \gamma) := \gamma/J^{-1}(1/a\gamma)$. Here p_c is also used to denote $p_c(a, \gamma)$. We now derive $p_c''(\theta)$ such that a connected $G_{n,r}$ becomes fully active for $p > p_c''$ whp. Observe that $p_c = p_c'(\theta) = p_c''(\theta)$.

Theorem 3 *Consider bootstrap percolation $BP(G_{n,r}, p, \theta)$ where $r = \sqrt{\pi^{-1}a \ln n}$ and $\theta = \gamma a \ln n$. For any $\gamma \in (0, 1/5\pi)$, $a \geqslant 5\pi/H(5\pi\gamma)$, and $p > p_c''(\theta) := p_c'' = \gamma/J^{-1}(1/a\gamma)$ where $J(x) = \ln x + x^{-1} - 1$ for $x \geqslant 1$, $G_{n,r}$ becomes fully active within $\mathcal{O}(n/r)$ steps whp.*

The proof consists of two parts. We tile the square $[0, \sqrt{n}]^2$ into cells $r/\sqrt{5} \times r/\sqrt{5}$ and show that in the initial configuration: (i) When $\gamma < 1/5\pi$ and $a \geqslant 5\pi/H(5\pi\gamma)$ every cell contains at least γD nodes whp, (ii) When $p > p_c''$ at least one cell contains γD or more active nodes. By Lemma 1 it follows that for a, γ, p in the specified ranges $G_{n,r}$ becomes fully active within $\mathcal{O}(n/r)$ steps whp.

Proof Tile the square $[0, \sqrt{n}]^2$ into cells $r/\sqrt{5} \times r/\sqrt{5}$, see Figure 5. Call two cells neighboring if they share one side. Notice every pair of nodes within the same cell or within two neighboring cells are adjacent by the choice of the size of a cell. Define $G_{n,r}'$

on the set of nodes of $G_{n,r}$ as follows. The set of edges of $G'_{n,r}$ consists of the subset of edges of $G_{n,r}$ whose terminal nodes belong to the same cell or two neighboring cells. By the monotonicity argument (Lemma 5 in Appendix)

$$\mathbb{P}_p\left(G'_{n,r} \text{ becomes fully active}\right) \leqslant \mathbb{P}_p\left(G_{n,r} \text{ becomes fully active}\right) . \tag{4}$$

Therefore it is sufficient to show that whp $G'_{n,r}$ becomes fully active when $p > p_c$ (10).

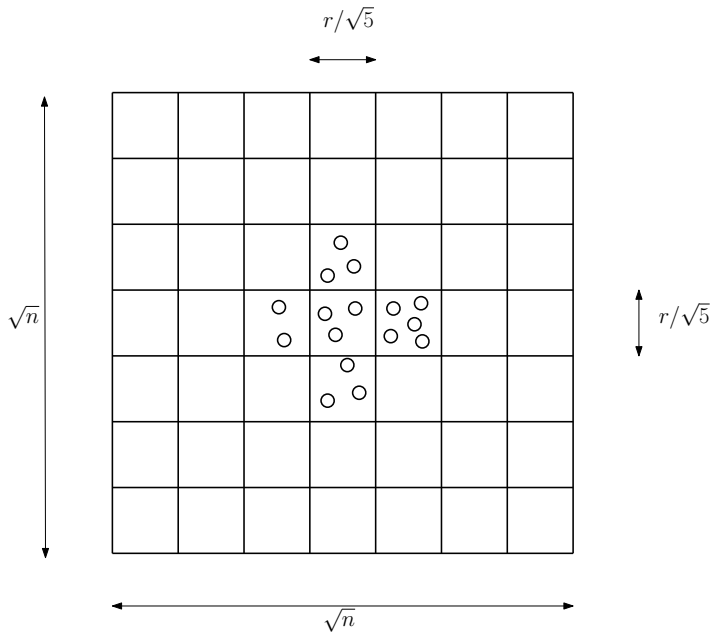

Figure 5: Tiling the square $[0, \sqrt{n}]^2$.

Part (i) (To show that every cell contains at least γD nodes whp.) We first bound the probability an arbitrary cell contains at least γD nodes. The number of nodes in a cell follows $\mathrm{Po}(r^2/5)$, i.e., $\mathrm{Po}(a \ln n/5\pi)$. Moreover, the numbers of nodes in cells are independent random variables (given the Poisson point process $\mathcal{X}$). For $\gamma < 1/5\pi$, from (12) we obtain

$$\begin{aligned}
\mathbb{P}\left(\text{a cell contains at most } \gamma D \text{ nodes}\right) &= \mathbb{P}\left(\mathrm{Po}\left(\frac{a \ln n}{5\pi}\right) < \gamma a \ln\right) \\
&\leqslant \exp\left(-\frac{a \ln n}{5\pi} H(5\pi\gamma)\right) \\
&= n^{-\frac{a}{5\pi} H(5\pi\gamma)} .
\end{aligned}$$

The total number of cells in $[0, \sqrt{n}]^2$ is $5n/r^2 = 5\pi n/(a \ln n) = o(n)$. The union bound taken over all cells yields

$$\mathbb{P}\left(\text{every cell contains at least } \gamma D \text{ nodes}\right) \geqslant 1 - o\left(n^{1-\frac{a}{5\pi}H(5\pi\gamma)}\right) . \tag{5}$$

Finally, for $a \geqslant 5\pi/H(5\pi\gamma)$, from (5) it follows that every cell contains at least γD nodes whp.

Part (ii). (To show that at least one cell contains γD or more active nodes.) We now derive conditions such that at least one cell contains at least $\theta = \gamma D$ active nodes in the initial configuration. In order to guarantee that whp there is at least one cell among $5n/r^2 = \Theta(n/\ln n)$, which contains at least θ active nodes in the initial configuration, it suffices to find p such that

$$\mathbb{P}\left(\mathrm{Po}(pD) \geqslant \gamma D + 1\right) = \omega\left(\frac{\ln n}{n}\right) , \tag{6}$$

since

$$\lim_{n\to\infty} 1 - (1 - \omega(\ln n/n))^{\Theta(n/\ln n)} = 1 .$$

Define $\alpha := (\gamma - p)/p$, then by rewriting (6) we need p such that

$$\mathbb{P}\left(\frac{\mathrm{Po}(pD) - pD}{pD} \geqslant \alpha + \frac{1}{pD}\right) = \omega\left(\frac{\ln n}{n}\right) . \tag{7}$$

By the Bahadur-Rao tail bound [3], as $n \to \infty$, i.e., $pD = \Theta(p \ln n) \to \infty$, the shifted Poisson random variable $\mathrm{Po}(pD) - pD$ satisfies

$$\mathbb{P}\left(\frac{\mathrm{Po}(pD) - pD}{pD} \geqslant \alpha\right) \approx \frac{\sqrt{1+\alpha}}{\alpha\sqrt{2\pi}} \frac{1}{\sqrt{pD}} \exp\left(-pDI(\alpha)\right) ,$$

where the *rate function* is defined by

$$I(\alpha) = \sup_{s\in\mathbb{R}} \{s\alpha - e^s + s + 1\} = (1+\alpha)\ln(1+\alpha) - \alpha . \tag{8}$$

Therefore for (7) to be satisfied we require

$$\frac{n}{\ln n} \frac{\sqrt{1+\alpha}}{\alpha\sqrt{2\pi}} \frac{1}{\sqrt{pD}} \exp\left\{-pDI(\alpha)\right\} = \omega(1) . \tag{9}$$

The left hand side of (9) equals

$$\begin{aligned} & \exp\left\{ \ln \frac{\sqrt{1+\alpha}}{\alpha\sqrt{2\pi}} - paI(\alpha)\ln n - \ln(pa\ln n) + \ln n - \ln\ln n \right\} \\ = \quad & \exp\left\{ (1 - apI(\alpha))\ln n - \ln(pa) - 2\ln\ln n + \ln \frac{\sqrt{1+\alpha}}{\alpha\sqrt{2\pi}} \right\} , \end{aligned}$$

which is $\omega(1)$ if $1 > apI(\alpha)$.

From (8) and $\alpha = (\gamma - p)/p$, the condition $1 > apI(\alpha)$ is equivalent to $1/a\gamma > J(\gamma/p)$, and moreover to

$$p > \frac{\gamma}{J^{-1}(1/a\gamma)} = p_c\,. \tag{10}$$

To complete the proof notice that once any γD nodes within a cell become active, all nodes within that cell become active at the next time step as would all nodes within its neighboring cells. This resulting process which jointly activates all nodes within one cell is equivalent to activating a site in $\mathbb{Z}^2$. The resulting BP in $\mathbb{Z}^2$ has the threshold $\theta = 1$ by construction, see Figure 5. Thus $BP(G'_{n,r}, p, \theta)$ becomes fully active when $p > p_c$ by Lemma 1. Now the proof follows from (4). □

3.2 Analysis of the Critical Threshold

The critical threshold $p_c = \gamma/J^{-1}(1/a\gamma)$ can be rewritten as

$$\ln p_c = -\ln a - \ln\left((1/a\gamma)J^{-1}(1/a\gamma)\right)\,. \tag{11}$$

The function $-\ln\left(xJ^{-1}(x)\right)$ is monotonically decreasing in x, hence p_c is monotonically increasing in a and monotonically decreasing in γ. As an example we numerically compute and tabulate p_c for $\gamma = 1/20$ and different values of a in Table 1. In Figure 6, p_c is plotted as a function in a with precision 10^{-6} for different values of $\gamma \in \{1/70, 1/60, 1/50, 1/40, 1/30, 1/20\}$.

a	p_c
3	0.000023419757716
4	0.000124245966822
5	0.000339190630161
6	0.000664971634409
7	0.00107946930311
8	0.00155764675019
9	0.00207790224432
10	0.00262345487779
25	0.0101188498021
50	0.0174952120548

a	p_c
100	0.0246619916484
200	0.0308408415894
300	0.0338938242715
400	0.035809469627
500	0.0371585449017
600	0.0381763433375
700	0.0389805098623
800	0.0396369961599
900	0.040186431355
1000	0.0406552556763

Table 1: Critical threshold p_c for different values of a and $\gamma = 1/20$.

The experiments are performed on $G_{n,r}$ with $n = 15000$ nodes and $r = \sqrt{a \ln n/\pi}$ for $a \in \{10, 25, 50\}$ and $\gamma = 1/20$. On these instances of graphs, for each chosen value

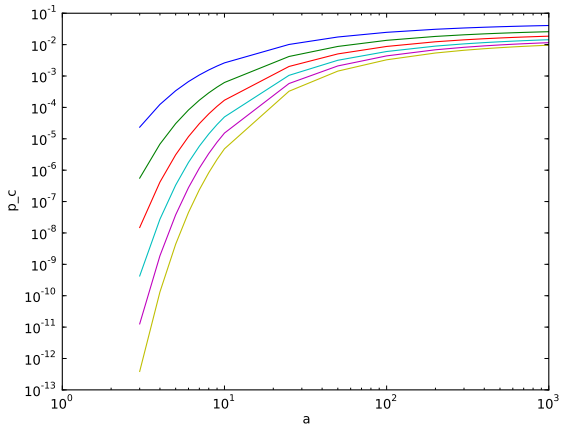

Figure 6: Critical threshold p_c for $\gamma \in \{1/70, 1/60, 1/50, 1/40, 1/30, 1/20\}$.

of p in $(0, 1)$ we simulate BP 100 times. More precisely, within each experiment we generate a random initial configuration with the probability p and perform BP with the threshold $\theta = \gamma D$ where the expected degree D is calculated for a given input $G_{n,r}$.

Our experimental results are presented such that abscissa corresponds to the initial probability p, while ordinate corresponds to the percentage of fully active stable configurations attained for a given p. The cases $a = 10, 25, 50$ are presented in Figure 7, Figure 8, Figure 9, respectively. A theoretical upper bound on the critical threshold p_c matches with the performed experiments, i.e., the instance of $BP(G_{n,r}, p, \theta)$ do not become fully active for $p < p_c(\theta)$. On the other hand instances of $BP(G_{n,r}, p, \theta)$ are expected to become fully active when $p > p_c(\theta)$. This, however, does not happen in our simulations when p is only slightly above $p_c(\theta)$. This is due to the finite size of $n = 15000$ in our simulations and for sufficiently large n we can verify every value of p strictly above the theoretical threshold $p_c(\theta)$. We do not know whether the analytically derived threshold is sharp and plan to examine this further.

Acknowledgements

This work was funded by NIST Grant No. 60NANB10D128.

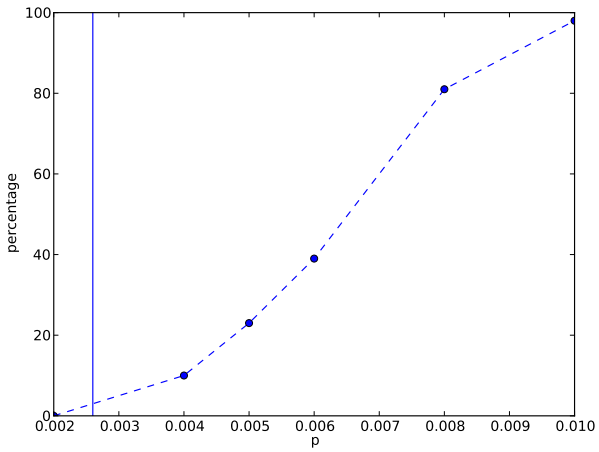

Figure 7: Percentage of fully percolated configurations in 100 simulations of $BP(G_{n,r}, p, \theta)$ when $n = 15000$, $r = \sqrt{10 \ln n / \pi n} \approx 0.0452$, $D = 10 \ln n \approx 96.16$ and $\theta = \lceil 20^{-1} \mathbb{E}(\deg) \rceil = \lceil 4.81 \rceil = 5$.

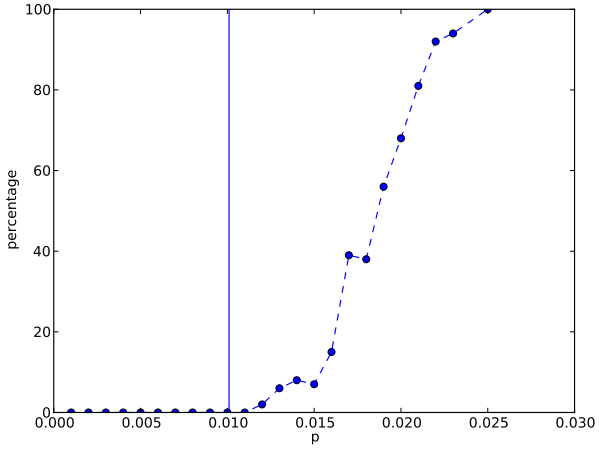

Figure 8: Percentage of fully percolated configurations in 100 simulations of $BP(G_{n,r}, p, \theta)$ when $n = 15000$, $r = \sqrt{25 \ln n / \pi n} \approx 0.0714$, $D = 25 \ln n \approx 240.40$ and $\theta = \lceil 20^{-1} \mathbb{E}(\deg) \rceil = \lceil 12.02 \rceil = 13$.

References

[1] AIZENMAN, M., AND LEBOWITZ, J. L. Metastability effects in bootstrap per-

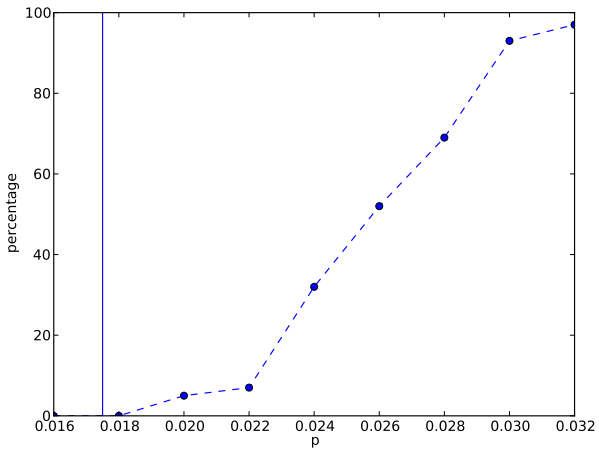

Figure 9: Percentage of fully percolated configurations in 100 simulations of $BP(G_{n,r}, p, \theta)$ when $n = 15000$, $r = \sqrt{50 \ln n/\pi n} \approx 0.1010$, $D = 50 \ln n \approx 480.79$ and $\theta = \lceil 20^{-1}\mathbb{E}(\deg) \rceil = \lceil 24.04 \rceil = 25$.

colation. *Journal of Physics A: Mathematical and General 21*, 19 (1988), 3801–3813.

[2] AMINI, H. Bootstrap percolation and diffusion in random graphs with given vertex degrees. *Electronic Journal of Combinatorics 17*, #R25 (2010).

[3] BAHADUR, R. R., AND RAO, R. R. On deviations of the sample mean. *Ann. Math. Statist. 31*, 4 (1960), 1015–1027.

[4] BALOGH, J., BOLLOBÁS, B., DUMINIL-COPIN, H., AND MORRIS, R. The sharp threshold for bootstrap percolation in all dimensions. In preparation.

[5] BALOGH, J., PERES, Y., AND PETE, G. Bootstrap percolation on infinite trees and non-amenable groups. *Combinatorics, Probability & Computing 15*, 5 (2006), 715–730.

[6] BALOGH, J., AND PITTEL, B. Bootstrap percolation on the random regular graph. *Random Structures & Algorithms 30*, 1-2 (2007), 257–286.

[7] CERF, R., AND CIRILLO, E. N. M. Finite size scaling in three-dimensional bootstrap percolation. *Ann. Prob 27* (1998).

[8] CHALUPA, J., LEATH, P. L., AND REICH, G. R. Bootstrap percolation on a Bethe lattice. *J. Phys. C 12*, L31 (1979).

[9] ERDŐS, P., AND RÉNYI, A. On random graphs. *Publ. Math. Inst. Hungar. Acad. Sci.* (1959).

[10] ERDŐS, P., AND RÉNYI, A. On the evolution of random graphs. *Publ. Math. Inst. Hungar. Acad. Sci.* (1960).

[11] GERSHO, A., AND MITRA, D. A simple growth model for the diffusion of new commuinication services. *IEEE Trans. on Systems, Man, and Cybernetics SMC-5*, 2 (March 1975), 209–216.

[12] GILBERT, E. N. Random graphs. *Ann. Math. Statist. 30*, 4 (1959), 1141–1144.

[13] GILBERT, E. N. Random plane networks. *Soc. Ind. Appl. Math. 9*, 4 (1961), 533–543.

[14] GOEL, A., RAI, S., AND KRISHNAMACHARI, B. Sharp thresholds for monotone properties in random geometric graphs. In *STOC '04: Proceedings of the thirty-sixth annual ACM symposium on Theory of computing* (New York, NY, USA, 2004), ACM Press, pp. 580–586.

[15] GUPTA, P., AND KUMAR, P. R. Critical power for asymptotic connectivity. In *Proceedings of the 37th IEEE Conference on Decision and Control* (1998), vol. 1, pp. 1106–1110.

[16] HOLROYD, A. E. Sharp metastability threshold for two-dimensional bootstrap percolation. *Probability Theory and Related Fields 125* (2003), 195–224.

[17] KONG, Z., AND YEH, E. M. Analytical lower bounds on the critical density in continuum percolation. In *Proceedings of the Workshop on Spatial Stochastic Models in Wireless Networks (SpaSWiN)* (Limassol, Cyprus, April 16, 2007.).

[18] LUCZAK, T., JANSON, S., TUROVA, T., AND VALLIER, T. Bootstrap percolation on the random graph $G_{n,p}$. *Ann. of Appl. Probab.* To appear.

[19] MEESTER, R., AND ROY, R. *Continuum percolation*. Cambridge University Press, 1996.

[20] PENROSE, M. D. The longest edge of the random minimal spanning tree. *The Annals of Applied Probability 7*, 2 (1997), 340–361.

[21] PENROSE, M. D. *Random Geometric Graphs*. Oxford University Press, 2003.

[22] POTTIE, G. J., AND KAISER, W. J. Wireless integrated network sensors. *Commun. ACM 43*, 5 (2000), 51–58.

[23] RINTOUL, M. D., AND TORQUATO, S. Precise determination of the critical threshold and exponents in a three-dimensional continuum percolation model. *Journal of Physics A. Mathematical and General 30*, 16 (1997), L585–L592.

[24] WATTS, D. J. A simple model of global cascades in random networks. *Proceedings of the National Academy of Sciences 99* (2002), 5766–5771.

Appendix

Lemma 4 *(Concentration on a Poisson random variable, see [21]). A Poisson random variable* $\mathrm{Po}(\lambda)$ *(with* $\lambda > 0$*) satisfies:*

$$\mathbb{P}\left(\mathrm{Po}(\lambda) > k\right) \leqslant \exp\left(-\lambda H(k/\lambda)\right), \text{ for } k > \lambda, \tag{12}$$

$$\mathbb{P}\left(\mathrm{Po}(\lambda) < k\right) \leqslant \exp\left(-\lambda H(k/\lambda)\right), \text{ for } k < \lambda, \tag{13}$$

where $H(x) = \ln x + x^{-1} + 1$ *for* $x > 0$.

Lemma 5 *For any two graphs* $G' = (V, E')$ *and* $G = (V, E)$ *on the same set of nodes* V *such that sets of edges satisfy* $E' \subseteq E$ *we have*

$$\mathbb{P}_p\left(G' \text{ becomes fully active}\right) \leqslant \mathbb{P}_p\left(G \text{ becomes fully active}\right).$$

Proof We prove the assertion by induction in t. Let X_v (respectively Y_v) be the first time when a node v becomes active in G' (respectively in G). For every $v \in V$ we have $\mathbb{P}_p\left(X_v = 0\right) = \mathbb{P}_p\left(Y_v = 0\right) = p$. Let us assume $\mathbb{P}_p\left(X_v = \tau\right) = \mathbb{P}_p\left(Y_v = \tau\right)$ for any $\tau \leqslant t$ and any $v \in V$. Then

$$\mathbb{P}_p\left(X_v = t+1\right) = \mathbb{P}_p\left(X_v = t\right) + \left(1 - \mathbb{P}_p\left(X_v = t\right)\right) \Pi_{X_v}(t), \tag{14}$$

where

$$\Pi_{X_v}(t) = \sum_{\ell=\theta}^{|N_G(v)|} \sum_{I \subseteq V : |I| = \ell} \prod_{i \in I} \mathbb{P}_p\left(X_v = t\right) \prod_{i \notin I} \left(1 - \mathbb{P}_p\left(X_v = t\right)\right).$$

Analogously we write the equation for $\mathbb{P}_p\left(X_v = t+1\right)$ and define $\Pi_Y(t)$

$$\mathbb{P}_p\left(Y_v = t+1\right) = \mathbb{P}_p\left(Y_v = t\right) + \left(1 - \mathbb{P}_p\left(Y_v = t\right)\right) \Pi_{Y_v}(t), \tag{15}$$

where

$$\Pi_{Y_v}(t) = \sum_{\ell=\theta}^{|N_G(v)|} \sum_{I \subseteq V : |I| = \ell} \prod_{i \in I} \mathbb{P}_p\left(Y_v = t\right) \prod_{i \notin I} \left(1 - \mathbb{P}_p\left(Y_v = t\right)\right) .$$

It is not hard to see that the inductive hypothesis $\mathbb{P}_p\left(X_v = t\right) \leqslant \mathbb{P}_p\left(Y_v = t\right)$ for any v and $N_{G'}(v) \subseteq N_G(v)$ yields

$$\Pi_{X_v}(t) \leqslant \Pi(t) . \tag{16}$$

Now (14), (15), and (16) give $\mathbb{P}_p\left(X_v = t+1\right) \leqslant \mathbb{P}_p\left(Y_v = t+1\right)$ for any v. Finally the initial configurations (at $t = 0$) satisfy $\mathbb{P}_p\left(\{X_v\}_{v \in V}\right) = \mathbb{P}_p\left(\{Y_v\}_{v \in V}\right)$ for $\{X_v\}_{v \in V} = \{Y_v\}_{v \in V}$, which concludes the proof. □